Journal of Alloys and Compounds 509 (2011) 3526–3531

Contents lists available at ScienceDirect

Journal of Alloys and Compounds

journal homepage: www.elsevier.com/locate/jallcom

Microstructure and mechanical properties of Mg–6Zn–*x*Cu–0.6Zr (wt.%) alloys

H.M. Zhu[a,b], G. Sha[b], J.W. Liu[a], C.L. Wu[c,*], C.P. Luo[a], Z.W. Liu[b], R.K. Zheng[b], S.P. Ringer[b]

[a] School of Materials Science and Engineering, South China University of Technology, Guangzhou 510640, China
[b] Australian Centre for Microscopy and Microanalysis, The University of Sydney, NSW 2006, Australia
[c] Center of High Resolution Electron Microscopy, School of Materials Science and Engineering, Hunan University, Changsha 410082, China

ARTICLE INFO

Article history:
Received 3 December 2010
Received in revised form
19 December 2010
Accepted 22 December 2010
Available online 28 December 2010

Keywords:
Mg alloys
Cu addition
Precipitate microstructure
Age-hardening
Mechanical properties

ABSTRACT

The microstructures and mechanical properties of the new quaternary Mg–6Zn–*x*Cu–0.6Zr alloys (*x* = 0, 0.5, 1.0 and 2.0 wt.%) have been investigated. The results show that the Cu content has a significant effect on the age-hardening response, tensile performance and fracture behavior of the alloys. The addition of 0.5 wt.% Cu resulted in a remarkable age-hardening response and a striking improvement of the room temperature tensile properties after an isothermal ageing at 180 °C. However, an excessive Cu addition of 2.0 wt.% caused the formation of continuous brittle grain-boundary intermetallic particles, thus degrading the age-hardening response and the mechanical properties of the alloy. The microstructural factors associated with the improvements in the mechanical properties are discussed in detail.

1. Introduction

As the lightest metallic structural materials, Mg alloys have attracted the worldwide research attentions over recent decades for their potential applications in the aerospace, aircraft and automotive industries [1]. Among the commercial Mg alloys available, Mg–Zn based alloys are of particular interest due to their pronounced age-hardening effects [2–5]. However, the predominant strengthening β_1' precipitates are widely reported to exhibit a coarse and inhomogeneous distribution within the matrix of the binary Mg–Zn alloy [2–5]. Effective control of the size and distribution of these precipitates is therefore crucial to ultimately produce Mg–Zn alloys with excellent mechanical properties.

Copper (Cu) is an important alloying element to Mg alloys. According to Unsworth [3] and Buha [4], the Cu addition can considerably improve the castability and age-hardening response of Mg–Zn alloys. The addition of a fourth alloying element, such as Mn, Al and Si, has been reported to exert a strong influence on the mechanical properties of the Mg–Zn–Cu alloy system [3]. For instance, a 0.5 wt.% Mn addition improves the yield strength at the expense of the reduced tensile strength and elongation [3]. Typical Cu contents in fully heat-treated Mg–6Zn–*x*Cu–0.5Mn alloys range from 1.5% to 3%, with the ultimate tensile strength (UTS) of 230–240 MPa, 0.2% proof yield strength (YS) of 160–170 MPa and elongation of 3–6%, respectively [3]. While this strength level is generally satisfactory and of technological interest, the ductility level is not practical for many applications, especially when the harmful effects of Cu on the corrosion resistance of Mg alloys are also considered. In this research, a new quaternary alloy of Mg–Zn–Cu–Zr is reported. The addition of Zirconium (Zr), as the fourth alloying element, is to refine the gain sizes [5] and to improve corrosion resistance of the alloys [6]. The present paper is aimed at the effects of Cu concentration on the age-hardening response and mechanical properties of the Mg–Zn–Cu–Zr alloys, so as to optimize the Cu addition and to develop a leaner, low cost high performance Mg alloy.

2. Experimental procedures

Commercially high purity Mg, Zn and Mg–28.78 wt.% Cu and Mg–31.63 wt.% Zr master alloys were used to prepare the Mg–6Zn–*x*Cu–0.6Zr alloys (*x* = 0, 0.5, 1.0, 2.0 wt.%) by casting in a permanent mold. The compositions were measured using an inductively coupled plasma spectrometer (ICP), and were very close to the nominal values. Throughout this paper, all alloy compositions are provided as wt.%. Based on the Mg–Zn–(Cu) phase diagram and the results of our recent differential scanning calorimetry (DSC) experiments [7], the Cu-free alloy was solution treated at 380 °C and the Cu-containing alloys were solution treated at 430 °C. All the alloys were solution treated for 24 h. Subsequently, the water quenched specimens were aged in an oil bath at 180 °C for times ranging up to 120 h.

Vickers hardness measurements were performed using a SHIMADZU HMV-2T microhardness tester with a load of 100 g and a holding time of 20 s. Tensile tests were conducted using a standard electronic universal testing machine (CMT 1505) at a crosshead speed of 1 mm/min. The tensile specimens, with a gauge length of 30 mm and a diameter of 5 mm, were fabricated from the peak-aged alloys. At least three tests were performed for each condition of interest. The tensile fracture

* Corresponding author.
E-mail addresses: cuilan-wu@163.com, cuilanwu2010@gmail.com (C.L. Wu).

0925-8388/$ – see front matter © 2010 Elsevier B.V. All rights reserved.
doi:10.1016/j.jallcom.2010.12.165

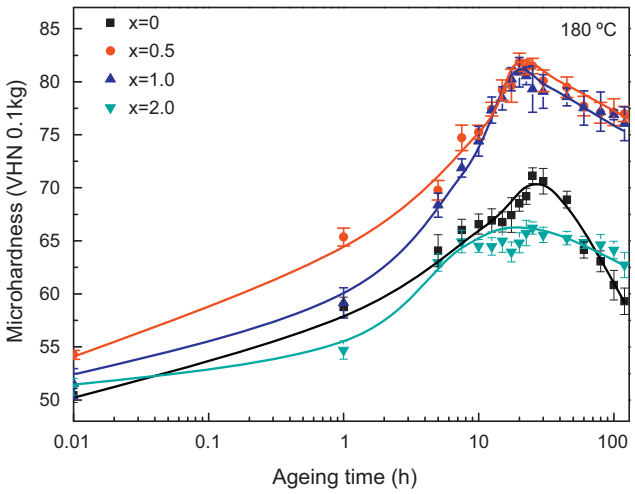

Fig. 1. Vickers hardness of the Mg–6Zn–*x*Cu–0.6Zr alloys against ageing time at 180 °C.

surfaces and the solutionized microstructures were examined by a Philips LEO 1530 VP scanning electron microscope (SEM) with an attached Oxford energy dispersive X-ray spectrometer (EDX) operated at 20 kV. X-ray diffraction (XRD) measurements were performed using a Philips X-PERT X-ray diffractometer with Cu Kα radiation at 40 mA and 40 kV. Transmission electron microscopy (TEM) was performed using a Phillips CM120 microscope operated at 120 kV. TEM thin foils were prepared by a twin-jet electropolishing method in a solution of 10.6 g LiCl, 22.32 g $Mg(ClO_4)_2$, 200 ml 2-butoxy-ethanol and 1000 ml methanol at about −45 °C and 70 V.

3. Results

3.1. Microhardness measurements of the alloys

The age-hardening profiles of the Mg–6Zn–*x*Cu–0.6Zr alloys are shown in Fig. 1. In the initial as-quenched condition, the hardness of the Cu-containing alloy decreased slightly with increasing Cu content but was still higher than that of the Cu-free alloy. When exposed to the subsequent ageing treatment, all these alloys exhibited an age-hardening behavior. Apparently, the age-hardening responses of the Cu-modified alloys with 0.5% and 1.0% Cu additions were significantly enhanced, with the peak hardness of ~82 VHN as compared to that of ~71 VHN for the Cu-free base alloy. Moreover, the time to reach the peak hardness was 20 h, shorter than 25 h for the Cu-free alloy. After ageing for 120 h, the hardness of the Mg–6Zn–(0.5, 1.0)Cu–0.6Zr alloys remains at 76 VHN, which is ~29% higher than the corresponding 59 VHN of the ternary Mg–6Zn–0.6Zr alloy. This indicates that microalloying with Cu delays the over-ageing in this alloy system. With further increasing the Cu content up to 2.0%, however, the corresponding age-hardening kinetic decreased obviously with a peak hardness of only 66 VHN.

3.2. Tensile properties and fractography of the alloys

Fig. 2 shows the typical stress–strain curves of the peak-aged Mg–6Zn–*x*Cu–0.6Zr alloys tested at room temperature. Their tensile properties including UTS, YS and elongation to failure are listed in Table 1. The addition of 0.5% Cu yielded the optimal mechanical properties, i.e. UTS of 266.3 MPa, YS of 185.6 MPa and elongation of 16.7%. With the addition of 1.0% Cu, the tensile properties of the resultant alloy decreased slightly but were still higher than those of the Cu-free base alloy. Apparently, a higher addition of 2.0% Cu substantially deteriorated the room temperature tensile performance of the alloy.

The fracture surfaces of the studied alloys were examined after tensile testing and the results are shown in Fig. 3. The

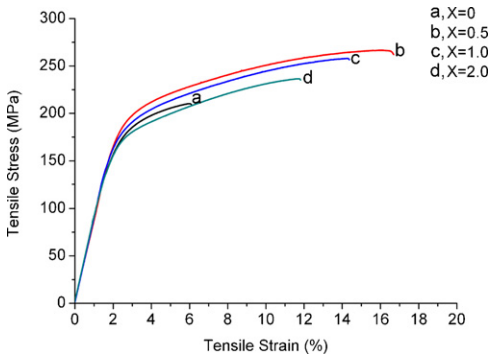

Fig. 2. Stress–strain curves of the peak-aged Mg–6Zn–*x*Cu–0.6Zr alloys.

Mg–6Zn–0.6Zr base alloy exhibits a distinctly brittle and intergranular cracking morphology (Fig. 3a). In contrast, the fracture surfaces of the Cu-modified alloys contain many dimples and tearing ridges as well as some cleavage steps and river patterns, which are characteristics of a mixture of quasi-cleavage and ductile fracture (Figs. 3b–d). The fractography observation is in good agreement with the high tensile elongation observed in the Cu-modified alloys. Examination at a higher magnification reveals the presence of bright particles, as marked by arrows in the inset of Fig. 3b. EDS analysis indicates that the Mg:Zn:Cu atomic ratio of such particles is approximately 64:17:19, confirming that they are MgZnCu-type intermetallics. The higher fraction of Mg in the EDS measurement could be due to the contribution of the Mg matrix. It is probably that the MgZnCu particles were the nucleation sites of microcracks formed by a void nucleation and coalescence mechanism when the alloys were subjected to the extensive plastic deformation. This suggestion is consistent with much more bright MgZnCu particles present in the fractured surfaces and the deteriorated tensile properties of the Mg–6Zn–*x*Cu–0.6Zr alloys with a higher Cu content.

3.3. Phase identifications of the alloys

Fig. 4 provides the XRD profiles from the Mg–6Zn–*x*Cu–0.6Zr alloys in the peak-aged condition. The profile from the Cu-free Mg–6Zn–0.6Zr alloy includes peaks from the hexagonal α-Mg matrix and the $MgZn_2$ phase. In contrast, additional diffraction peaks were observed for the Cu-containing alloys. Following comparison with the International Centre for Diffraction Data (ICDD, #65-7003), the cubic MgZnCu phase was identified. TEM examination as shown in Fig. 5 confirmed that the particle at the grain-boundary is indeed the cubic MgZnCu with its [1 0 0] diffraction pattern inserted in the figure. The MgZnCu intermetallic compound is a Laves phase of the C15 $MgCu_2$ type and possesses a high melting point and good thermal stability [8]. It is expected that the presence of this ternary interdendritic Laves phase can suppress the sliding of the grain boundary at elevated temperature and thus enhance the high-temperature performance of the Cu-containing alloys.

Table 1
The room-temperature tensile properties of the Mg–6Zn–*x*Cu–0.6Zr alloys in the peak-aged condition.

Alloys	Ultimate tensile strength (UTS, MPa)	0.2% yield strength (YS, MPa)	Elongation (%)
Mg–6Zn–0.6Zr	209.4	153.2	6.1
Mg–6Zn–0.5Cu–0.6Zr	266.3	185.6	16.7
Mg–6Zn–1.0Cu–0.6Zr	257.8	167.4	13.4
Mg–6Zn–2.0Cu–0.6Zr	236.1	152.1	11.6

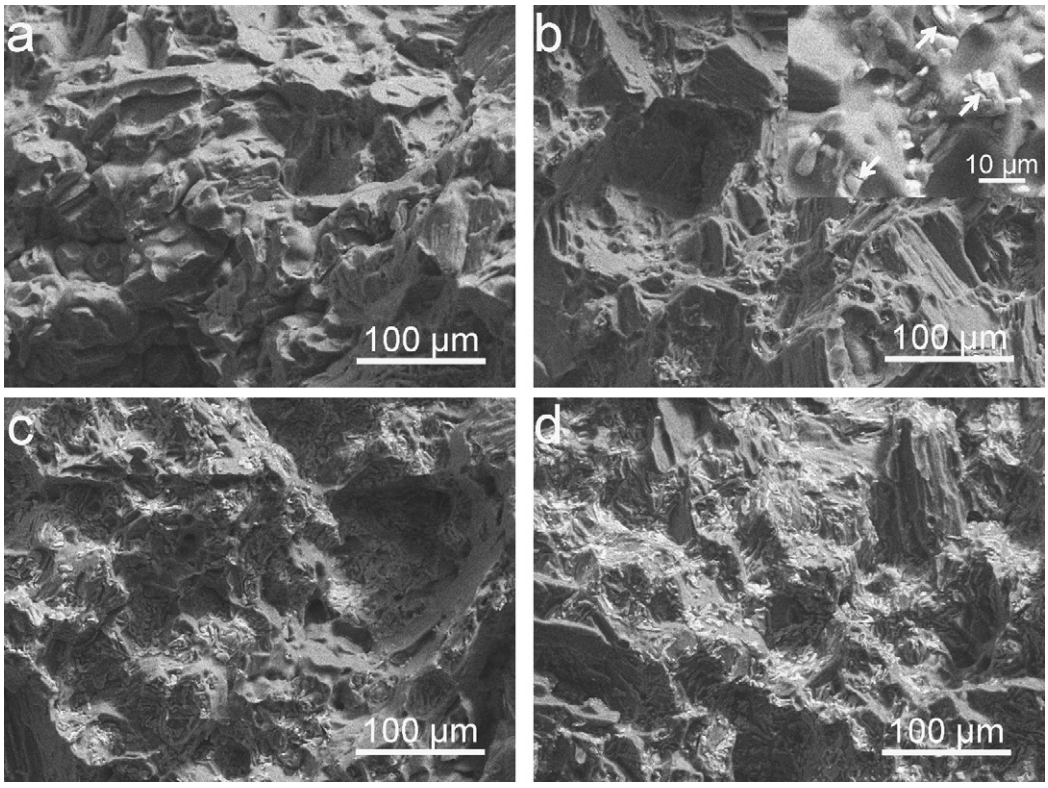

Fig. 3. SEM images of the tensile fractographs for the peak-aged Mg–6Zn–*x*Cu–0.6Zr alloys tested at room temperature (a) $x = 0$; (b) $x = 0.5$; (c) $x = 1.0$; (d) $x = 2.0$.

3.4. Microstructures of the alloys

Fig. 6 shows the SEM backscattered electron images of the solution treated Mg–6Zn–*x*Cu–0.6Zr alloys with different Cu additions. Two types of coarse particles with different morphologies exist in the Cu-containing alloys. The globular particles are binary $Mg_{51}Zn_{20}$ (or Mg_7Zn_3) phases and dominant in the Cu-free alloy. Similar particles have been commonly observed in Mg–Zn-based alloys [4]. The coarse elongated particles are MgZnCu intermetallics according to EDX analysis and mainly distributed along the grain boundary of the Cu-containing alloys, as marked by arrows in Fig. 6b. Since the solubility of Cu in Mg matrix is very low (0.31–0.55 wt.% in pure Mg at 440 °C [4]), it is not surprising that more MgZnCu particles were observed with increasing Cu addition as shown in Fig. 6. Similar observations were made from the fractography examination (Fig. 3) and XRD results (Fig. 4) described previously.

TEM micrographs in $[1\,1\,\bar{2}\,0]_\alpha$ zone axis of the peak-aged Mg–6Zn–*x*Cu–0.6Zr alloys are compared in Fig. 7. Similar to the previous investigations on various Mg–Zn based alloys [2–4], two types of precipitates are clearly visible in the Cu-free Mg–6Zn–0.6Zr alloy. One is β_1' rods perpendicular to $(0\,0\,0\,1)_\alpha$ plane and the other is β_2' plates parallel to $(0\,0\,0\,1)_\alpha$ plane, as indicated in Fig. 7a. The precipitate microstructures of the Cu-free base alloy are extremely not uniform. The size and number density of these precipitates vary among different grains and even within the same grain. The inho-

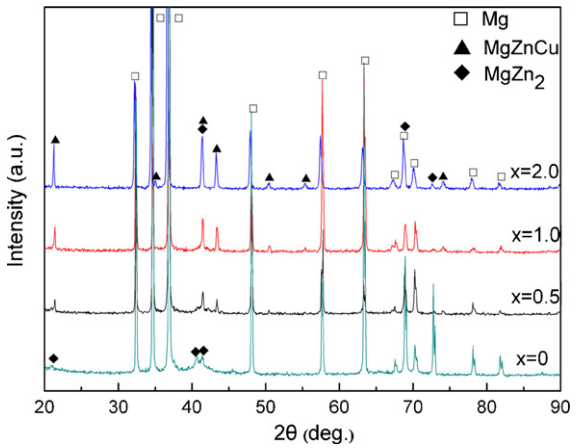

Fig. 4. XRD pattern of the peak-aged Mg–6Zn–*x*Cu–0.6Zr alloys.

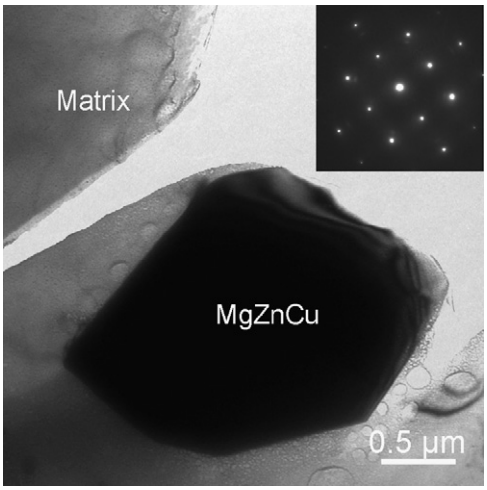

Fig. 5. TEM micrograph of a representative interdentric MgZnCu particle. Inset image is the corresponding selected area diffraction pattern recorded along $[1\,0\,0]_{MgZnCu}$ direction.

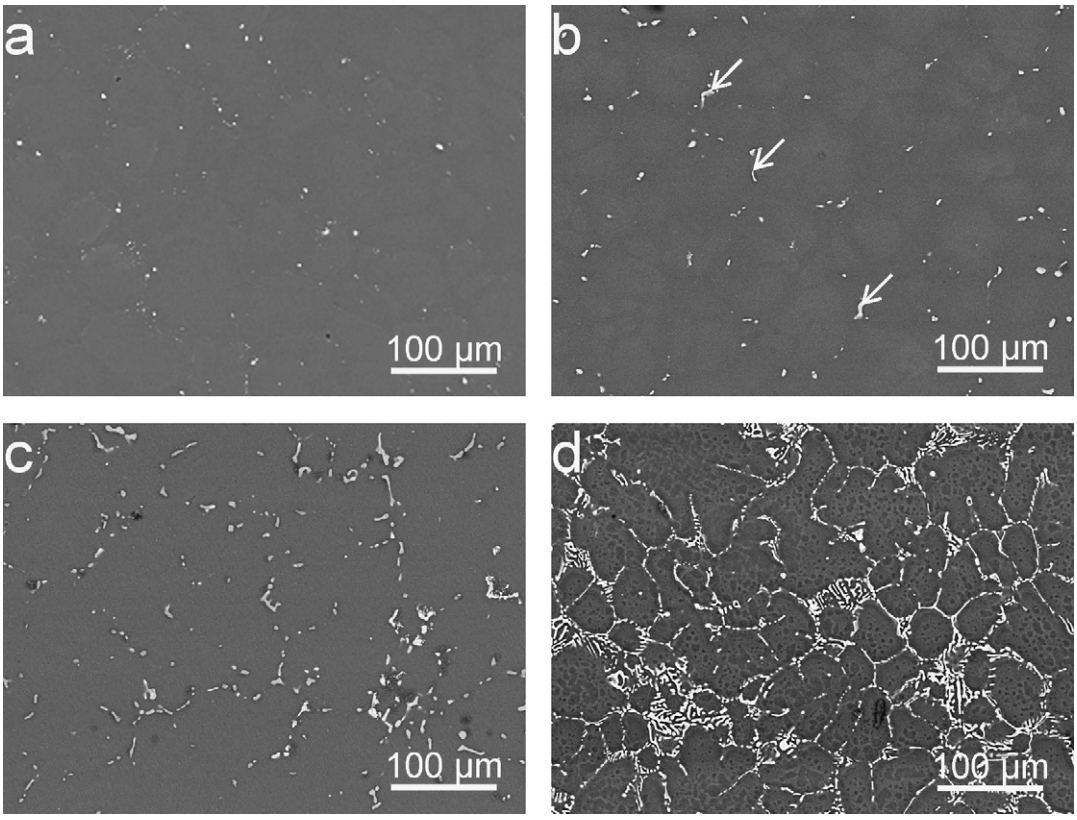

Fig. 6. SEM images of Mg–6Zn–*x*Cu–0.6Zr alloys after solutionization treatments (a) $x = 0$; (b) $x = 0.5$; (c) $x = 1.0$; (d) $x = 2.0$.

mogeneous distribution of precipitates was also widely observed in similar alloys [2–4]. In marked contrast, the 0.5% Cu addition to the Mg–6Zn–0.5Zr alloy resulted in a significantly uniform distribution of the rod-like β_1' precipitates (Fig. 7b). With the increase of Cu addition, the aspect ratios of β_1' precipitates decreased remarkably as seen in Figs. 7b–d. The average aspect ratio (~9:1) of β_1' precipitates in the alloy with a 2.0% Cu addition is about five times lower than ~53:1 observed in the alloy with a 0.5% Cu addition. In addition, fewer $(0\,0\,0\,1)_\alpha$ β_2' plates were observed in the Cu-containing alloys.

4. Discussion

4.1. Effects of Cu on the microstructure and age-hardening response of the alloys

The micro-alloying element (Cu) produced a remarkable influence on precipitation in the Mg–6Zn–0.6Zr base alloy. As illustrated in Fig. 7, the inhomogeneous distribution of the dominant β_1' precipitates was significantly eliminated in the Cu-modified alloys. This can probably be attributed to the increased number of homogeneously and densely dispersed stable nuclei in the Cu-containing alloys [4]. Concomitantly, the occurrence of $(0\,0\,0\,1)_\alpha$ β_2' precipitates associated with the onset of over-ageing was retarded in the Cu-modified alloy. This result suggests that Cu could postpone the over-ageing effect of the Mg–6Zn–0.6Zr alloy, which is consistent with the slow decrease in hardness of the Cu-modified alloys after a longer ageing treatment as seen in Fig. 1.

It should be noted that although the micro-alloying Cu has a potential to increase the eutectic temperature of the Mg–Zn based alloy and permits the use of a higher solution temperature to maximize the solubility of the solute element Zn [3,4], a portion of Zn solute atoms can be consumed due to the formation of the MgZnCu intermetallics in the Cu-containing alloys. With the increased MgZnCu particles in the alloys with a higher Cu content, the Zn concentration in the solid solution was substantially reduced for further precipitation. Consequently, the decreased number density and aspect ratio of the dominant $[0\,0\,0\,1]_\alpha$ β_1' precipitates led to a poor age-hardening response of the Mg–6Zn–2.0Cu–0.6Zr alloy as shown in Fig. 1.

4.2. Effects of Cu on the tensile properties of the alloys

It is a significant finding in this study that a 0.5% Cu addition into the Mg–6Zn–0.6Zr alloy yields the optimum tensile properties, i.e. a combination of high strength and excellent ductility. This is likely due to the fact that the Cu addition promotes the homogeneous precipitation of $[0\,0\,0\,1]_\alpha$ β_1' rods and retards the occurrence of $(0\,0\,0\,1)_\alpha$ β_2' precipitates, as shown in Fig. 7. Consequently, the Cu-modified alloy demonstrated a good tensile performance (Table 1). It is known that the microstructural inhomogeneity has been an issue in many binary Mg–Zn alloys [3,4]. The Cu addition can potentially offer a valuable solution to the problem for these alloys. TEM examinations as shown in Fig. 7 demonstrate that the trace Cu addition (i.e. 0.5% and 1.0%) enhanced the formation of the predominant strengthening β_1' precipitates in high number densities and high aspect ratios. These long thin $[0\,0\,0\,1]_\alpha$ β_1' rod precipitates provide a much stronger barrier to block the dislocation movement on the $(0\,0\,0\,1)_\alpha$ basal slip plane than the short β_1' rods and the $(0\,0\,0\,1)_\alpha$ β_2' precipitates [9]. Thus, we can conclude that the effective modification of precipitate microstructure is responsible for the improved tensile strengths of the Mg–6Zn–(0.5, 1.0)Cu–0.6Zr alloys. However, a higher addition of Cu at 2.0% has caused the excess formation of the MgZnCu intermetallics, and thus reduced the amount of Zn available for the formation of rod-like β_1' precipitates with an extremely low aspect ratio during ageing treatment.

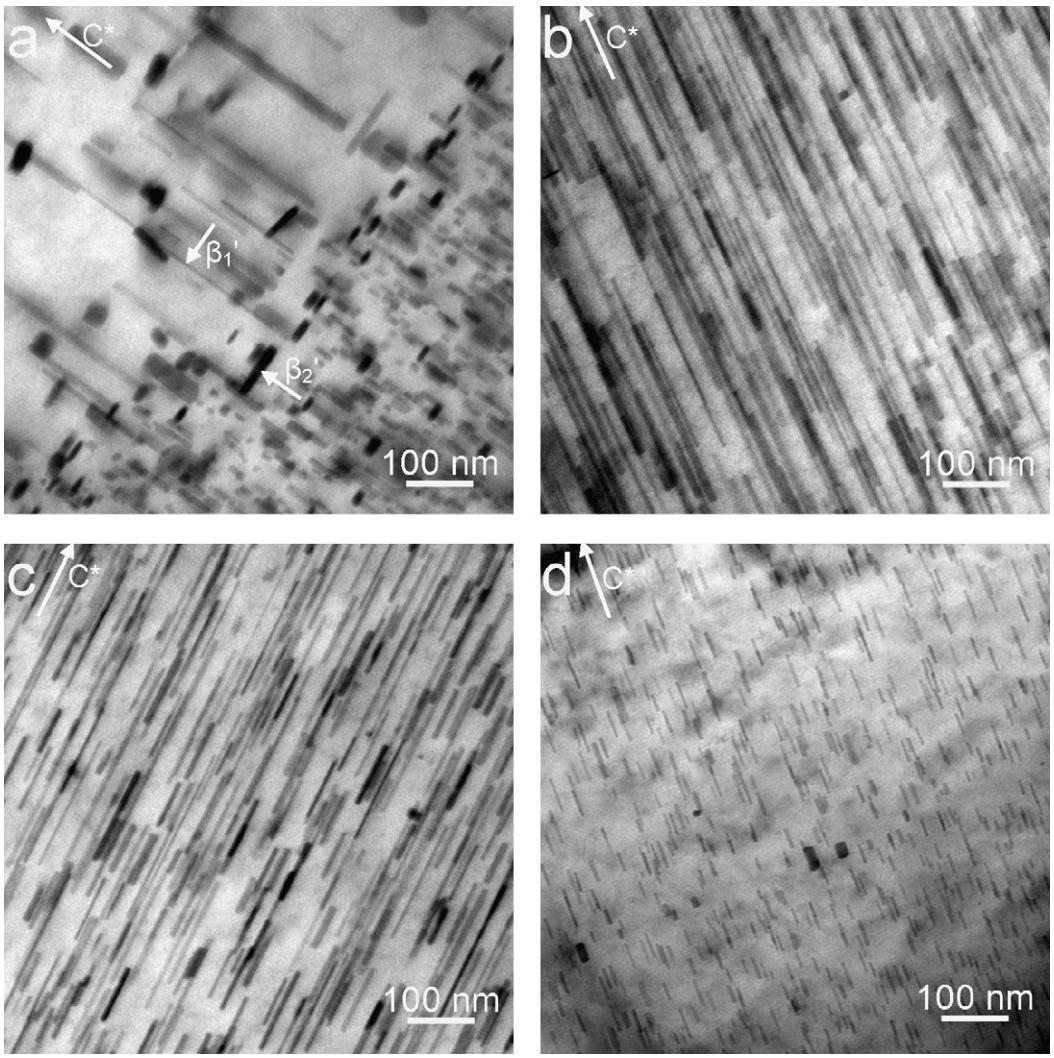

Fig. 7. TEM bright field images of the peak-aged Mg–6Zn–*x*Cu–0.6Zr alloys along the $[1\,1\,\bar{2}\,0]_\alpha$ zone axis. (a) $x = 0$; (b) $x = 0.5$; (c) $x = 1.0$; (d) $x = 2.0$.

This explains why the alloy with 2.0% Cu shows an inferior tensile performance.

The Mg–6Zn–(0.5, 1.0)Cu–0.6Zr alloys exhibit an attractively high elongation of above 13%. Two main factors including grain size [10] and *c*/*a* axial ratio [11–14] have been considered having a great influence on the elongation of cast magnesium alloys. Since the grain size of the Cu-containing alloys shows no clear change (Fig. 6), the high elongations are unlikely due to the grain size refinement. It is well-known that some alloying elements such as Li [13,14] and Ca [14] can reduce the *c*/*a* ratio of magnesium and thus stimulate the activation of non-basal slips to facilitate the room-temperature plastic deformation. For example, an as-cast Mg–4.0Zn–0.5Ca alloy has been reported having a large elongation of 17% due to its low *c*/*a* ratio [14]. Interestingly, Ganeshan et al. [11] recently reported a *c*/*a* reduction value of 0.657% for Mg–Cu alloy, 0.525% for Mg–Li alloy and 0.201% for Mg–Ca alloy by first-principles calculations and all these alloys exhibited enhanced ductility by micro-alloying. A rough estimation from our XRD results indicates the *c*/*a* reduction value for Mg–6Zn–(0, 0.5, 1.0, 2.0)Cu–0.6Zr alloys is 0.006%, 0.345%, 0.285% and 0.169%, respectively. It is therefore probable that the enhanced ductility of our Cu-modified alloys could partially due to the reduced *c*/*a* ratio by the Cu addition.

In general, Cu did change the precipitation behavior of the strengthening phases β_1' and β_2' and thus affected the strengthening response of the alloys. When in a range of 0.5–1.0 wt.%, Cu addition can optimize the mechanical properties of the alloys by (1) increasing the number density and aspect ratio of the dominant strengthening phase β_1', and (2) retarding the precipitation of the less effective β_2' for strengthening, though the mechanism by which Cu behaves this way is unclear at present. When the Cu addition reaches 2.0 wt.%, however, the mechanical properties are seen to deteriorate, because (1) the formation of continuous brittle grain-boundary MgZnCu intermetallic particles occurs, which would consume a large part of Zn needed to form the strengthening β_1', as well as Cu needed to affect the precipitation behavior of β_1', thus reducing the number density and aspect ratio of β_1'; and (2) the grain-boundary phase MgZnCu itself would have embrittled the alloys.

5. Conclusions

Additions of Cu have significant effects on the precipitate microstructure, mechanical properties and fracture mechanism of Mg–6Zn–*x*Cu–0.6Zr alloys.

(1) For Cu additions in the range of 0.5–1.0 wt.%, the optimal age-hardening response during isothermal ageing at 180 °C and room-temperature tensile properties were recorded. Of par-

ticular interest is the excellent tensile elongation of over 13%. The Cu additions in this range have promoted a more uniform distribution of the rod-like β_1' precipitates along the $[0\,0\,0\,1]_\alpha$ direction.

(2) For Cu addition up to 2.0 wt.%, a continuous precipitation of embrittling grain-boundary MgZnCu intermetallic particles occurs together with rod-like β_1' precipitates with a relatively low number density and aspect ratio. These microstructures are responsible for the alloy having poor age-hardening response and inferior mechanical properties.

(3) The Cu-free base alloy showed a typical intergranular brittle fracture while the Cu-modified alloys exhibited a mixed fracture of quasi-cleavage with ductile rupture characterized by dimples and tear ridges.

Acknowledgements

This project is supported by National Basic Research (973) Program of China (No. 2009CB623704) and Nature Science Foundation of Guangdong Province, China (No. 07006483). H.M. Zhu would like to acknowledge the financial support from the China Scholarship Council (CSC). The authors also acknowledge the facilities, scientific and technical assistance from AMMRF at the University of Sydney, particularly, Drs. Dave Mitchell and Ting-Yu Wang.

References

[1] B.L. Mordike, T. Ebert, Mater. Sci. Eng. A 302 (2001) 37–45.
[2] X. Gao, J.F. Nie, Scripta Mater. 56 (2007) 645–648.
[3] W. Unsworth, Light Met. Age 45 (1987) 10–13.
[4] J. Buha, T. Ohkubo, Metall. Mater. Trans. A 39 (2008) 2259–2273.
[5] M. Shahzad, L. Wagner, J. Alloys Compd. 486 (2009) 103–108.
[6] M. Sun, G.H. Wu, W. Wang, W.J. Ding, Mater. Sci. Eng. A 523 (2009) 145–151.
[7] H.M. Zhu, C.P. Luo, J.W. Liu, Z.W. Liu, S.P. Ringer, Mater. Sci. Forum 654–656 (2010) 655–658.
[8] Y. Liu, G.Y. Yuan, C. Lu, W.J. Ding, Trans. Nonferrous Met. Soc. China 17 (2007) s353–357.
[9] J.F. Nie, Scripta Mater. 48 (2003) 1009–1015.
[10] S.M. He, L.M. Peng, X.Q. Zeng, W.J. Ding, Y.P. Zhu, Mater. Sci. Eng. A 433 (2006) 175–181.
[11] S. Ganeshan, S.L. Shang, Y. Wang, Z.K. Liu, Acta Mater. 57 (2009) 3876–3884.
[12] F.H. Herbstein, B.L. Averbach, Acta Metall. 4 (1956) 407–413.
[13] A. Becerra, M. Pekguleryuz, J. Mater. Res. 23 (2008) 3379–3386.
[14] A.L. Geng, B.P. Zhang, A.B. Li, C.C. Dong, Mater. Lett. 63 (2009) 557–559.